Multiwavelength excitation Raman scattering of Cu2ZnSn(SxSe1x)4 (0x1) polycrystalline thin films: Vibrational properties of sulfoselenide solid solutions

Mirjana Dimitrievska, Haibing Xie, Andrew Fairbrother, Xavier Fontané, Galina Gurieva, Edgardo Saucedo, Alejandro Pérez-Rodríguez, Susan Schorr, and Victor Izquierdo-Roca

Citation: Applied Physics Letters **105**, 031913 (2014); doi: 10.1063/1.4891333
View online: http://dx.doi.org/10.1063/1.4891333
View Table of Contents: http://scitation.aip.org/content/aip/journal/apl/105/3?ver=pdfcov
Published by the AIP Publishing

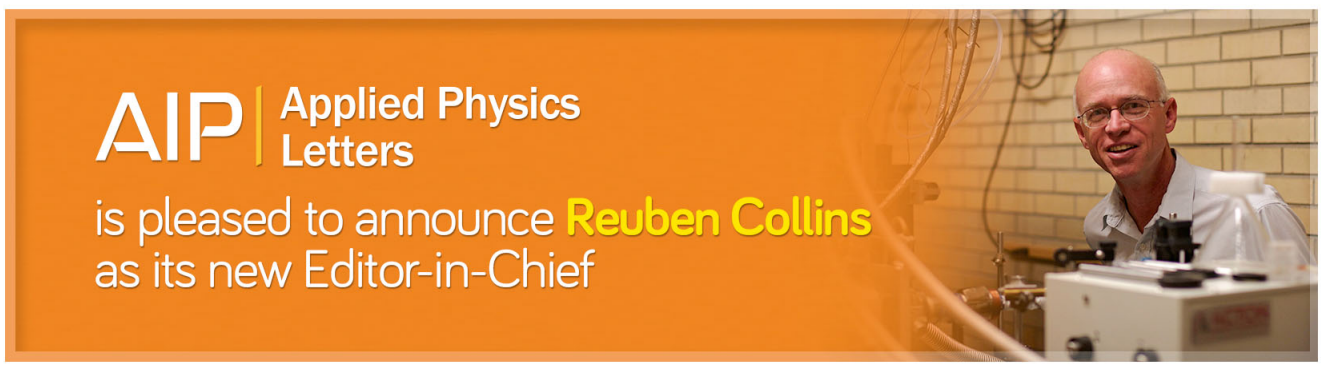

Multiwavelength excitation Raman scattering of $Cu_2ZnSn(S_xSe_{1-x})_4$ ($0 \le x \le 1$) polycrystalline thin films: Vibrational properties of sulfoselenide solid solutions

Mirjana Dimitrievska,[1] Haibing Xie,[1] Andrew Fairbrother,[1] Xavier Fontané,[1] Galina Gurieva,[2] Edgardo Saucedo,[1] Alejandro Pérez-Rodríguez,[1,3] Susan Schorr,[2,4] and Victor Izquierdo-Roca[1,a)]

[1]*Catalonia Institute for Energy Research (IREC), Jardins de les Dones de Negre 1 2pl., 08930 Sant Adrià del Besòs, Barcelona, Spain*
[2]*Helmholtz Centre Berlin for Materials and Energy, Department Crystallography, Hahn-Meitner-Platz 1, 14109 Berlin, Germany*
[3]*IN²UB, Departament d'Electrònica, Universitat de Barcelona, C. Martí i Franquès 1, 08028 Barcelona, Spain*
[4]*Institute of Geological Sciences, Freie Universität Berlin, Malteserstr. 74-100, 12249 Berlin, Germany*

(Received 10 June 2014; accepted 14 July 2014; published online 23 July 2014)

In this work, Raman spectroscopy and X-ray diffraction were applied together to evaluate the crystal structure and the phonon modes of photovoltaic grade $Cu_2ZnSn(S_xSe_{1-x})_4$ thin films, leading to a complete characterization of their structural and vibrational properties. Vibrational characterization has been based on Raman scattering measurements performed with different excitation wavelengths and polarization configurations. Analysis of the experimental spectra has permitted identification of 19 peaks, which positions are in good accord with theoretical predictions. Besides, the observation of Cu_2ZnSnS_4-like A symmetry peaks related to S vibrations and $Cu_2ZnSnSe_4$-like A symmetry peaks related to Se vibrations, additional Raman peaks, characteristic of the solid solution and previously not reported, are observed, and are attributed to vibrations involving both S and Se anions. © *2014 AIP Publishing LLC*. [http://dx.doi.org/10.1063/1.4891333]

Kesterite Cu_2ZnSnS_4 (CZTS) and $Cu_2ZnSnSe_4$ (CZTSe) compounds and their solid solutions $Cu_2ZnSn(S_xSe_{(1-x)})_4$ (CZTSSe) have attracted much attention due to their potential application in thin film solar cells as light absorber materials. In contrast with more mature thin film technologies based on $Cu(InGa)Se_2$ chalcopyrites, these compounds are only composed of earth abundant and non-toxic elements. So far the best devices are based on Se-rich CZTSSe absorbers, with the reported record efficiency of 12.6%.[1] Although devices based on CZTSSe solid solutions exhibit the highest solar cells efficiencies, their structural and vibrational properties have been studied considerably less than the ones corresponding to the quaternary CZTS and CZTSe counterparts.

To date the majority of studies reported on the CZTSSe compounds deal mainly with different synthesis processes and their influence on optoelectronic properties (solid state reaction,[2] co-evaporation,[3] sputtering deposition,[4] monograin molten-salt synthesis,[5] colloidal nanocrystal syntheses,[6] hydrazine,[1] and non-hydrazine based solution processing[7]). Several groups have also confirmed the ability to tune the bandgap of CZTSSe solid solutions by control of stoichiometry which allows for more versatile tuning of optical properties.[2–6] Systematic variation of the sulfur/selenium ratio allows the bandgap to be tuned from 1.4 to 0.9 eV, which greatly extends potential application of CZTSSe alloys in thin film photovoltaic devices, where a defined and controllable bandgap is required. Theoretical calculations, based on first principles simulations, of the band structure and optical properties of CZTSSe compounds have revealed that the mixed-anion alloys are highly miscible.[8] Furthermore, the composition dependence of structure and optical properties of CZTSSe powders has been experimentally investigated in Ref. 2, where a linear decrease of lattice parameters in accordance with Vegard's law was observed with the change in composition from S-rich to Se-rich samples. As for the vibrational properties, experimental determination of the main Raman scattering vibrational modes has been done in Refs. 2–6, where usually the two-mode behavior was attributed to the most intensive modes throughout the entire alloy concentration range. Additionally, weaker peaks were interpreted as secondary phases such as SnS, SnSe, ZnS, and ZnSe or Se.

In order to further develop CZTSSe thin film solar cells and achieve better device performance and higher efficiencies, a deeper knowledge on the fundamental and vibrational properties of these compounds and their impact on the optoelectronic parameters are required.

Herein Raman spectroscopy and X-ray diffraction (XRD) are applied together to perform a systematic study of the crystal structure and the phonon modes of the polycrystalline CZTSSe device grade layers (used for producing solar cells with up to 8.2% efficiency). This has allowed a detailed characterization of the structural and vibrational properties in the complete range of anion compositions of the solid solutions ($0 \le S/(S+Se) \le 1$). Furthermore, for better identification of Raman modes and their dependence on the anion composition Raman measurements with different excitation wavelengths from ultra-violet (UV) to near-infrared (NIR) regions are performed. NIR excitation conditions are used due to the expected increase in the intensity of the Raman modes because of near-resonant Raman effects. This is expected to take place, in

a)Email: vizquierdo@irec.cat

particular, for the polar modes of CZTS–like peaks, which are NIR active and are usually observed as very weak peaks in standard Raman scattering conditions.[9] The analysis of the experimentally obtained spectra has allowed observation of the existence of a more complex behavior than the two-mode behavior previously reported for these solid solutions.

CZTSSe device grade layers were synthesized on Mo coated soda-lime glass by annealing of Cu/Sn/Cu/Zn metallic multi-stacks, deposited by DC magnetron sputtering, under a S + Se + Sn atmosphere. Changing the mass of S and Se and the total pressure during the annealing, it was possible to tune the S-Se composition in the whole range, from pure CZTS to pure CZTSe.[4] The cationic ratios of Cu/(Sn + Zn) and Zn/Sn were kept constant between 0.75–0.80 and 1.16–1.22, respectively. As grown S-rich samples were submitted to an HCl etching[10] and Se-rich ones to a two stage $KMnO_4/H_2SO_4 + Na_2S$ (Ref. 11) etching with the aim to remove ZnS(Se) secondary phases potentially present at the surface of the absorbers. Raman scattering measurements performed with excitation conditions corresponding to resonant excitation of ZnS and ZnSe phases confirms the absence of these phases on the surface of the etched samples.[11,12]

Solar cells were fabricated with these layers as described in Ref. 4. Optoelectronic properties from the devices synthesized in this way gave efficiencies up to 8.2%. External quantum efficiency (EQE) curves were obtained using a PV300 Photovoltaic characterization system (Bentham Instruments).

Raman scattering measurements were performed in back scattering configuration with a LabRam HR800-UV and T64000 Horiba-Jobin Yvon spectrometers. For the HR800-UV system, diode-pumped solid state lasers with wavelengths of 785.0 and 532.0 nm and gas HeCd laser with wavelength of 325.0 nm were used for excitation. In this system, excitation and light collection were made through an Olympus metallographic microscope with a laser spot diameter of the order of 1–2 μm, depending on the excitation wavelength. To avoid effects in the spectra related to potential microscopic inhomogeneities, the spot was rastered over an area of $30 \times 30\ \mu m^2$. Furthermore, the T64000 system works coupled with an ion-Ar + laser, and measurements were made with 514.5 nm and 457.9 nm excitation lines, with a 100 μm spot size on the sample. In all cases, and to avoid the presence of thermal effects in the spectra, the power excitation density on the surface of the samples was around 50 W/cm^2. Under these experimental measurement conditions no thermal effects are observed in the spectra. This has been corroborated by the analysis of spectra measured with different excitation powers. The first-order Raman spectrum of monocrystalline Si was measured as a reference before and after acquisition of each Raman spectrum, and the spectra were corrected with respect to the Si line at 520 cm^{-1}.

XRD diffraction patterns were measured on PANalytical X'pert Pro MPD diffractometer with Cu−Kα-radiation ($\lambda = 1.54056$ Å) and a secondary graphite monochromator. Structural characterization of the thin films was carried out by grazing incidence XRD (GIXRD) with angles of 0.5°, 1°, 2°, and 5°. Refinements of the lattice constant values were carried out by Le Bail analysis using the FullProf[13] program with Thompson-Cox-Hastings pseudo-Voigt convoluted with axial divergence asymmetry profile function.[14]

The crystal structure of CZTSSe solid solutions was characterized by XRD measurements from which representative patterns of the 112 reflection are presented in Figure 1(a). The anion compositions of the samples were obtained based on the position of the 112 diffraction peak in comparison with the positions of this peak for the pure CZTS and CZTSe compounds. The systematic shift in peak position towards higher angles as the S/(S + Se) ratio increases correlates with the replacement of smaller S atoms with larger Se atoms. Furthermore, presence of a single and symmetric 112 diffraction peak in all measured diffractograms indicates that all samples are homogeneously alloyed rather than a mixture of CZTS and CZTSe phases.[15] The kesterite structure (space group $I\bar{4}$) was used as starting model for the refinement procedure, since it has been shown that both CZTS and CZTSe adopt a kesterite structure.[16] Additionally, lattice parameters *a* and *c* of the thin films were obtained as result of the Le Bail analysis. The dependence of lattice parameters on S/(S + Se) ratio is presented in the inset in Figure 1 and it is in good accordance with the Vergard's law.

In order to examine the compositional uniformity through the thickness of CZTSSe thin films, GIXRD measurements with 0.5°, 1°, 2°, and 5° angles were performed. Inset in Figure 1(b) presents diffractograms measured from S-rich and Se-rich samples. No significant shift in peak positions of the 112 reflection with the change in grazing incidence angles was observed. Additionally lattice parameters obtained from Le Bail analysis and presented in Figure 1(b), have proven to be constant for all grazing incidence angles. Furthermore, Raman measurements preformed on the front and back surface of the layers do not show changes in the

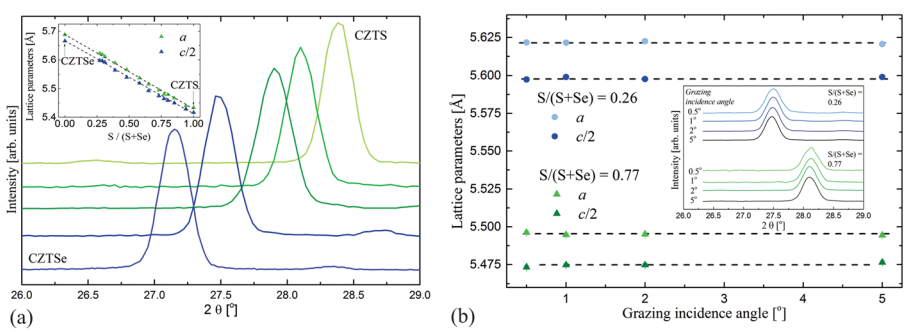

FIG. 1. (a) Representative XRD diffractograms centered at the 112 reflection kesterite peak measured for CZTSSe solid solutions. Inset: Lattice parameters on dependence of the anion S/(S + Se) composition ratio. (b) Lattice parameters in dependence of grazing incidence angles for two representative samples with 0.26 and 0.77 S/(S + Se) composition. Inset: Representative GIXRD diffractograms centered at the 112 reflection kesterite peak measured with 0.5°, 1°, 2°, and 5° angles for CZTSSe samples with 0.26 and 0.77 S/(S + Se) compositions.

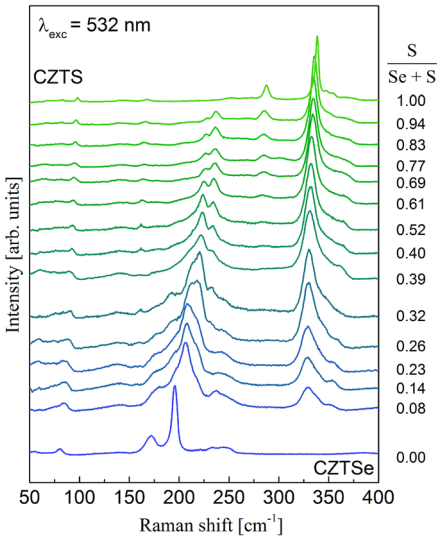

FIG. 2. Raman spectra of polycrystalline CZTSSe solid solution thin films measured with a 532.0 nm excitation wavelength.

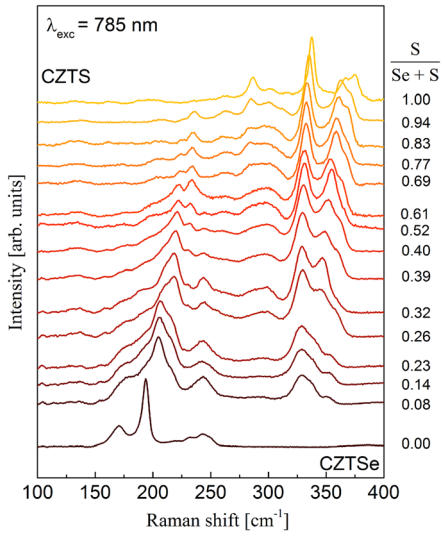

FIG. 4. Raman spectra of polycrystalline CZTSSe solid solution thin films measured with a 785.0 nm excitation wavelength.

shape and positions of Raman peaks. Raman measurements from the back region were made with the laser spot directly focused on the back surface of the layer from layers that were previously mechanically removed from the substrate.[17] This behavior strongly supports the absence of the significant changes in the S/(S + Se) composition through the thickness of the layers, thus the CZTSSe thin films used in this study could be considered uniform.

Irreducible representation of the kesterite structure with the space group $I\bar{4}$ ($\Gamma = 3A \oplus 6B \oplus 6E$) leads to the theoretical prediction of 27 active Raman modes, from which most have been experimentally detected for the CZTS and CZTSe compounds.[9,18] Usually, two dominant Raman peaks have been observed in this system and assigned to A symmetry modes. On the other hand, the CZTSSe compounds have a more complex behavior as seen in Figure 2, which presents Raman spectra of series of samples with different S/(S + Se) compositions measured with a 532 nm excitation wavelength.

Figure 3(a) presents the frequencies of the most intense Raman peaks of CZTSSe solid solutions plotted against composition. Note that Raman scattering is a surface sensitive technique (penetration depth of approximately ~100 nm in CZTSSe), which is why the surface anion compositions of the samples used for Raman characterization are calculated based on the Vergard's law applied on the bandgap energies which were determined from EQE measurements of solar cell devices based on these films. This is because the penetration depth of scattered light is similar to the expected width of the space charge region in the devices. Anion compositions obtained from the EQE measurements are in good agreement with the compositions obtained from the XRD measurements.

The Raman spectra of CZTSSe solid solutions are characterized by the presence of two dominant peaks in the higher frequency region (280–400 cm^{-1}) and two dominant peaks in the lower frequency region (170–205 cm^{-1}). The peaks in the higher frequency region are identified with CZTS-like peaks corresponding to A symmetry modes involving pure S vibrations,[9] and the peaks in the lower frequency region are identified with CZTSe-like peaks corresponding to A symmetry modes involving pure Se vibrations.[18,19] This apparently agrees with the existence of a two-mode behavior for these peaks, as previously reported in Refs. 2–6.

In addition, the Raman spectra from the solid solutions also show additional peaks in the intermediate frequency region (205–280 cm^{-1}). The observed additional peaks could not be attributed to secondary phases, because measurements with the 325.0 and 457.9 nm excitation wavelengths have demonstrated the absence of ZnS and ZnSe secondary phases or their alloys, which are resonant under these conditions.[11,12] Furthermore, the spectral contributions of Sn-(S,Se) phases are expected in the 50–220 cm^{-1} interval,[20,21] which is not completely overlapping with the frequency interval of the observed additional peaks. Finally, the experimental conditions under which the samples were prepared, constituted of Zn-rich and

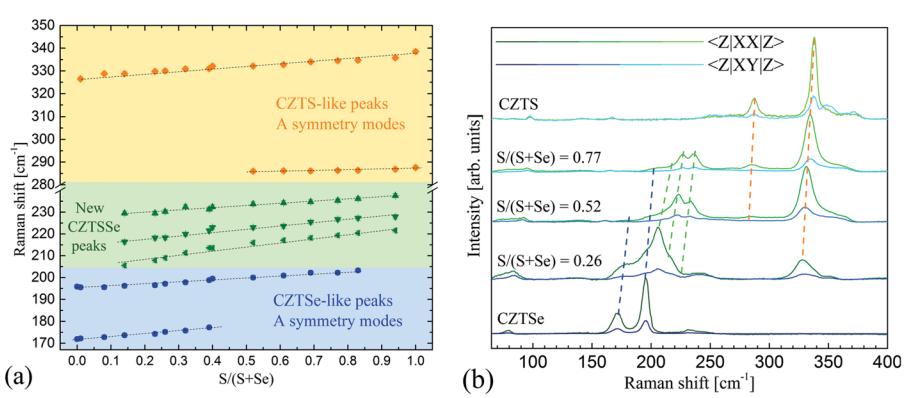

FIG. 3. (a) Variations of the frequencies of the most intense Raman peaks of CZTSSe solid solutions on dependence of S/(S + Se) anion composition ratio. (b) Raman polarization measurements of CZTSSe solid solutions done in parallel and perpendicular polarization configurations (excitation wavelength of 514.5 nm). Dashed lines are visual guide for the most intense Raman peaks positions presented in Figure 3(a).

Cu-poor conditions, are expected to inhibit formation of detrimental Cu-Sn-(S,Se) ternary phases and Cu-(S,Se) binary phases.[22] The absence of these phases is also confirmed by the XRD measurements. All this leads to the conclusion that the additional peaks are due to vibrational modes involving vibrations of both S and Se anions in the lattice. Accordingly, the vibrational spectrum from the solid solution is more complex than the previously reported two-mode behaviour. Similar behaviour in the Raman modes of alloys with the appearance of additional peaks was also observed in Cu-(S,Se) system.[23]

From Figure 3(a), all observed Raman modes shift monotonously with the variation of the composition and no splitting of peaks are detected. These results suggest that the observed Raman spectra of CZTSSe compounds of the intermediate compositions are able to be interpreted based on the kesterite type structure, which is in accordance with XRD results. As the cationic ratios were kept constant for all samples, it is expected that changes in the peak positions are caused mainly by the change in anion composition. Additional CZTSSe peaks in the interval of 205–280 cm^{-1} show a higher dependency of frequency from the anion composition ratio than the CZTS-like and CZTSe-like ones, which indicates that they are attributable to vibrational modes which include vibrations from both S and Se atoms in the lattice, in contrast with CZTS-like or CZTSe-like peaks that involve vibrations of only one kind of anion. Furthermore, full-width-at-half-maximum (FWHM) of peaks from the solid solution are similar to those observed in the pure compounds, which indicates the absence of significant chemical disorder effects.[24] These results suggest the possible existence of fine ordering of anions in the structure, instead of the expected random distribution.

TABLE I. Frequency (in cm^{-1}) of peaks from simultaneous fitting of Raman spectra of CZTSSe solid solutions for different S/(S + Se) anion compositions measured with 532.0 and 785.0 nm excitation wavelengths. The proposed symmetries of the modes are determined based on polarization measurements, resonant Raman measurements, and comparison with the modes of the pure S and Se kieserite compounds reported in Refs. 9 and 18 (/ is assignment of the overlapped modes).

Experimentally reported in Ref. 18		This work						Experimentally reported in Ref. 9	
S/(S + Se) = 0		S/(S + Se) = 0.26		S/(S + Se) = 0.52		S/(S + Se) = 0.77		S/(S + Se) = 1	
RS[a] (cm^{-1})	Sym[b]	RS[c] (cm^{-1})	Sym[d]	RS[c] (cm^{-1})	Sym[d]	RS[c] (cm^{-1})	Sym[d]	RS[e] (cm^{-1})	Sym[f]
		58.9	E	60.8	E	62.7	E	67.8	E
		69.9	B	75.7	B	75.8	B	81.5	B
77	B	76.4	B	85.4	B	85.8	B		
82	E	83.8	E	92.6	E	92.9	E	96.9	E/B
138	E	131.1	E	139.4	E	139.3	E	139.8	E
		140.4		146.3		145.3			
157	B	153.7	B	163.0	B	162.9	B	164.1	B
170	A								
174	A	175.0	A						
				176.0		174.5			
178	B	180.8							
196	A	196.6	A	200.7	A	202.9	A		
		208.2	A or B	214.8	A or B	219.4	A or B		
		217.0	A or B	223.3	A or B	226.7	A or B		
224	E								
231	E								
		230.5	A or B	234.4	A or B	235.1	A or B		
235	B	237.2	B/E	246.3	B/E	254.2	B/E	255.1	B/E
239	B	245.2	B	262.6	B	265.1	B	262.7	B
245	B								
250	B								
								271.1	E
				286.0	A	286.4	A	287.1	A
		290.3	A	300.5	A	301.0	A	302.1	A
								315.9	E
								331.9	B
		329.8	A	331.5	A	332.1	A	337.5	A
		334.0	B/E	345.0	B/E	346.8	B/E	347.3	E
								353.0	B
		352.4	B/E	357.9	B/E	358.3	B/E	366.6	E
								374.4	B

[a]RS is the Raman shift reported in Ref. 18.
[b]Sym is the symmetry reported in Ref. 18.
[c]RS is the Raman shift from this work.
[d]Sym is symmetry proposed in this work.
[e]RS is the Raman shift reported in Ref. 9.
[f]Sym is the symmetry reported in Ref. 9.

Raman polarization measurements performed on these layers (Figure 3(b)) show the same behavior for the additional peaks observed in the 205–280 cm^{-1} region as that of CZTS-like and CZTSe-like A symmetry peaks. According to Raman tensors for the space group $I\bar{4}$ and calculations of depolarization ratio for the polycrystalline films with random orientation, with changes in polarization conditions from parallel $\langle Z|XX|Z\rangle$ to perpendicular $\langle Z|XY|Z\rangle$ configurations the intensity of all A modes would always decrease, while the intensity of all E modes would always increase. In case of B modes, their intensity could increase or decrease depending on their type. Assuming the existence of a kesterite crystalline structure for the alloys (in agreement with the XRD data) and the expected behavior of the modes with the change in polarization conditions, this indicates that these peaks are related to either A or B symmetry modes.[9]

In order to deepen understanding of the CZTSSe vibrational modes and to more clearly observe and resolve the peaks, Raman measurements with a 785 nm excitation wavelength were performed on the same set of samples. The Raman spectra measured on the films with different compositions are plotted in Figure 4. The intensity of the Raman peaks located at highest frequencies from the spectra of S-rich CZTSSe samples are enhanced in the case of 785 nm excitation due to the resonance Raman effects. This kind of behavior is attributed to the coupling of the excitation energy with the electronic energy bands at Γ point.[9] The selective enhancement of these peaks suggests that they can be attributed to polar modes, since this kind of behavior is expected only for those type of modes,[9] which again, assuming the kesterite structure, indicates that these peaks are related to B or E symmetry modes.

The detailed simultaneous fittings of the experimental spectra with Lorentzian curves and polarization measurements have allowed identification of 19 peaks. The positions of the peaks are in good accordance with those calculated for these compounds from first principle simulations.[8] The position of each Raman peak for the three representative samples with $S/(S+Se)$ anion compositions of 0.26, 0.52, and 0.77 are presented in Table I. In this Table, the symmetry of the modes related to the different peaks is proposed based on the polarization and Raman scattering resonant measurements, and from the comparison with the previously reported experimental Raman modes from the CZTS[9] and CZTSe compounds.[18]

In conclusion, this work presents a complete vibrational characterization based on simultaneous fittings of the Raman spectra measured with different excitation wavelengths and under different polarization configurations, which allowed identification of 19 peaks. In contrast with previous reports on the existence of a two-mode behavior, a more complex behavior of the most intense peaks with the change in anion composition has been observed. The Raman spectra from the solid solution show dominant CZTS-like peaks in the higher frequency region (280–400 cm^{-1}), dominant CZTSe-like peaks in the lower frequency region (170–205 cm^{-1}), and additional peaks related to vibrations of both S and Se anions in the intermediate frequency region (205–280 cm^{-1}). These results provide a better insight in the fundamental properties of CZTSSe solar cells, and lead to an improved knowledge on their vibrational properties.

The research leading to these results has received funding from the People Program (Marie Curie Actions) of the European Union's Seventh Framework Program FP7/2007-2013/ under REA Grant Agreement No. 316488 (KESTCELLS). Authors from IREC and University of Barcelona belong to the M-2E (Electronic Materials for Energy) Consolidated Research Group and the XaRMAE Network of Excellence on Materials for Energy of the "Generalitat de Catalunya." A.F. thanks the Spanish Ministry of Economy and Competitiveness (MINECO) for the FPU Fellowship (FPU12/05508), V.I. for the "Juan de la Cierva" Fellowship (JCI-2011-10782), E.S. for the "Ramon y Cajal" Fellowship (RYC-2011-09212), and H.X. thanks support from the "China Scholarship Council" fellowship (CSC No. 201206340113).

[1]W. Wang, M. T. Winkler, O. Gunawan, T. Gokmen, T. K. Todorov, Y. Zhu, and D. B. Mitzi, Adv. Energy Mater. **4**, 1301465 (2014).
[2]J. He, L. Sun, S. Chen, Y. Chen, P. Yang, and J. Chu, J. Alloys Compd. **511**, 129 (2012).
[3]L. Grenet, S. Bernardi, D. Kohen, C. Lepoittevin, S. Noël, N. Karst, A. Brioude, S. Perraud, and H. Mariette, Sol. Energy Mater. Sol. Cells **101**, 11 (2012).
[4]A. Fairbrother, X. Fontané, V. Izquierdo-Roca, M. Espindola-Rodriguez, S. López-Marino, M. Placidi, J. López-García, A. Pérez-Rodríguez, and E. Saucedo, ChemPhysChem **14**, 1836 (2013).
[5]M. Grossberg, J. Krustok, J. Raudoja, K. Timmo, M. Altosaar, and T. Raadik, Thin Solid Films **519**, 7403 (2011).
[6]A. Singh, S. Singh, S. Levcenko, T. Unold, F. Laffir, and K. M. Ryan, Angew. Chem., Int. Ed. **52**, 9120 (2013).
[7]Y. Sun, Y. Zhang, H. Wang, M. Xie, K. Zong, H. Zheng, Y. Shu, J. Liu, H. Yan, M. Zhu, and W. Lau, J. Mater. Chem. A **1**, 6880 (2013).
[8]A. Khare, B. Himmetoglu, M. Cococcioni, and E. S. Aydil, J. Appl. Phys. **111**, 123704 (2012).
[9]M. Dimitrievska, A. Fairbrother, X. Fontané, T. Jawhari, V. Izquierdo-Roca, E. Saucedo, and A. Pérez-Rodríguez, Appl. Phys. Lett. **104**, 021901 (2014).
[10]A. Fairbrother, E. García-Hemme, V. Izquierdo-Roca, X. Fontané, F. A. Pulgarín-Agudelo, O. Vigil-Galán, A. Pérez-Rodríguez, and E. Saucedo, J. Am. Chem. Soc. **134**, 8018 (2012).
[11]S. López-Marino, Y. Sánchez, M. Placidi, A. Fairbrother, M. Espindola-Rodríguez, X. Fontané, V. Izquierdo-Roca, J. López-García, L. Calvo-Barrio, A. Pérez-Rodríguez, and E. Saucedo, Chem. - Eur. J. **19**, 14814 (2013).
[12]A. Fairbrother, X. Fontané, V. Izquierdo-Roca, M. Espíndola-Rodríguez, S. López-Marino, M. Placidi, L. Calvo-Barrio, A. Pérez-Rodríguez, and E. Saucedo, Sol. Energy Mater. Sol. Cells **112**, 97 (2013).
[13]J. Rodriguez-Carvajal and T. Roisnel, Physica B **192**, 55 (1993).
[14]L. W. Finger, D. E. Cox, and A. P. Jephcoat, J. Appl. Crystallogr. **27**, 892 (1994).
[15]P. M. P. Salomé, J. Malaquias, P. A. Fernandes, M. S. Ferreira, A. F. da Cunha, J. P. Leitão, J. C. González, and F. M. Matinaga, Sol. Energy Mater. Sol. Cells **101**, 147 (2012).
[16]S. Siebentritt and S. Schorr, Prog. Photovoltaics: Res. Appl. **20**, 512 (2012).
[17]S. Lopez-Marino, M. Placidi, A. Perez-Tomas, J. Llobet, V. Izquierdo-Roca, X. Fontane, A. Fairbrother, M. Espindola-Rodriguez, D. Sylla, A. Perez-Rodriguez, and E. Saucedo, J. Mater. Chem. A **1**, 8338 (2013).
[18]M. Guc, S. Levcenko, V. Izquierdo-Roca, X. Fontané, E. Arushanov, and A. Pérez-Rodríguez, J. Appl. Phys. **114**, 193514 (2013).
[19]N. B. M. Amiri and A. Postnikov, Phys. Rev. B **82**, 205204 (2010).
[20]L. S. Price, I. P. Parkin, A. M. E. Hardy, R. J. H. Clark, T. G. Hibbert, and K. C. Molloy, Chem. Mater. **11**, 1792 (1999).
[21]T. Fukunaga, S. Sugai, T. Kinosada, and K. Murase, Solid State Commun. **38**, 1049 (1981).
[22]A. Nagoya, R. Asahi, R. Wahl, and G. Kresse, Phys. Rev. B **81**, 113202 (2010).
[23]M. Ishii, K. Shibata, and H. Nozaki, J. Solid State Chem. **105**, 504 (1993).
[24]M. Dimitrievska, A. Fairbrother, A. Pérez-Rodríguez, E. Saucedo, and V. Izquierdo-Roca, Acta Mater. **70**, 272 (2014).